Journal of Visualized Experiments

FLIM-FRET measurements of protein-protein interactions in live bacteria.

--Manuscript Draft--

Article Type:	Invited Methods Article - JoVE Produced Video
Manuscript Number:	JoVE61602R1
Full Title:	FLIM-FRET measurements of protein-protein interactions in live bacteria.
Section/Category:	JoVE Biology
Keywords:	FRET-FLIM; protein-protein interactions; Pseudomonas aeruginosa; bacteria; imaging; fluorescence
Corresponding Author:	Julien Godet Universite de Strasbourg Illkirch, France FRANCE
Corresponding Author's Institution:	Universite de Strasbourg
Corresponding Author E-Mail:	julien.godet@unistra.fr
Order of Authors:	Hanna Manko
	Vincent Normant
	Quentin Perraud
	Tania Steffan
	Véronique Gasser
	Emmanuel Boutant
	Éleonore Réal
	Isabelle J. Schalk
	Yves Mély
	Julien Godet
Additional Information:	
Question	**Response**
Please indicate whether this article will be Standard Access or Open Access.	Standard Access (US$2,400)
Please indicate the **city, state/province, and country** where this article will be **filmed**. Please do not use abbreviations.	Strasbourg,Alsace,France

TITLE:

FLIM-FRET Measurements of Protein-Protein Interactions in Live Bacteria

AUTHORS AND AFFILIATIONS:

Hanna Manko[1], Vincent Normant[2,3], Quentin Perraud[2,3], Tania Steffan[1], Véronique Gasser[2,3], Emmanuel Boutant[1], Éléonore Réal[1], Isabelle J. Schalk[2,3], Yves Mély[1] and Julien Godet[1, 4, *]

[1]Université de Strasbourg, Laboratoire de Bioimagerie et Pathologies, UMR CNRS 7021, Illkirch, Strasbourg, France
[2]Université de Strasbourg, UMR 7242, ESBS, Bld Sébastien Brand, Illkirch, Strasbourg, France
[3]CNRS, UMR 7242, ESBS, Bld Sébastien Brand, Illkirch, Strasbourg, France
[4]Groupe Méthode Recherche Clinique, Hôpitaux Universitaires de Strasbourg, France

Email Addresses of Co-authors:
Hanna Manko (hanna.manko@etu.unistra.fr)
Vincent Normant (normant@unistra.fr)
Quentin Perraud (q.perraud@unistra.fr)
Tania Steffan (tania.steffan@unistra.fr)
Véronique Gasser (veronique.gasser@unistra.fr)
Emmanuel Boutant (emmanuel.boutant@unistra.fr)
Éléonore Réal (eleonore.real@unistra.fr)
Isabelle J. Schalk (isabelle.schalk@unistra.fr)
Yves Mély (yves.mely@unistra.fr)

Corresponding author:
Julien Godet (julien.godet@unistra.fr)

KEYWORDS:

FRET-FLIM, protein-protein interactions, *Pseudomonas aeruginosa*, bacteria, imaging, fluorescence

SUMMARY:

We describe here a protocol to characterize protein-protein interactions between two highly-differently expressed proteins in live *Pseudomonas aeruginosa* using FLIM-FRET measurements. The protocol includes bacteria strain constructions, bacteria immobilization, imaging and post-imaging data analysis routines.

ABSTRACT:

Protein-protein interactions (PPIs) control various key processes in cells. Fluorescence lifetime imaging microscopy (FLIM) combined with Förster resonance energy transfer (FRET) provide accurate information about PPIs in live cells. FLIM-FRET relies on measuring the fluorescence lifetime decay of a FRET donor at each pixel of the FLIM image, providing quantitative and accurate information about PPIs and their spatial cellular organizations. We propose here a detailed protocol for FLIM-FRET measurements that we applied to monitor PPIs in live

Pseudomonas aeruginosa in the particular case of two interacting proteins expressed with highly different copy numbers to demonstrate the quality and robustness of the technique at revealing critical features of PPIs. This protocol describes in detail all the necessary steps for PPI characterization - starting from bacterial mutant constructions up to the final analysis using recently developed tools providing advanced visualization possibilities for a straightforward interpretation of complex FLIM-FRET data.

INTRODUCTION:

Protein-protein interactions (PPIs) control various key processes in cells[1]. The roles of PPIs differ based on protein composition, affinities functions and locations in cells[2]. PPIs can be investigated via different techniques[3]. For example, co-immunoprecipitation is a relatively simple, robust, and inexpensive technique commonly used tool to identify or confirm PPIs. However, studying PPIs can be challenging when the interacting proteins have low expression levels or when the interactions are transient or relevant only in specific environments. Studying PPIs occurring between the different enzymes of the pyoverdine pathway in *P. aeruginosa* requires that the repression of the general iron-co-factored repressor Fur is relieved to allow the expression of all the proteins of the pyoverdine pathway to be expressed in the cell[4,5,6]. This common regulation for all the proteins of the pathway results in timely expressions in the cell expected to promote their interactions. The diversity in term of size, nature, expression levels and the number of proteins of this metabolic pathway make it difficult for study in reconstituted systems[6]. Exploring PPIs in their cellular environment is therefore critical to further understand the biological functions of proteins in their native context.

Only few methods including fluorescence allow exploring PPIs in living cells[7]. Amongst the different fluorescence parameters that can be measured, the fluorescence lifetime (i.e., the average time a fluorophore remains in its excited state before emitting a photon) is likely one of the most interesting parameters to explore in living cells. The fluorescence lifetime of a fluorophore is highly sensitive to its environment and FLIM can therefore provide chemical or physical information regarding the fluorophore surroundings[8]. This includes the presence of Förster resonance energy transfer (FRET) that can occur in the presence of an “acceptor” of fluorescence located at a short distance of a fluorescence “donor”. Energy transfer results in significant shortening of the donor fluorescence lifetime (**Figure 1A**), making Fluorescence Lifetime Imaging Microscopy (FLIM) a powerful approach to explore protein-protein interactions directly in live cells. FLIM can additionally provide spatial information about where the interactions take place in cells[7,8]. This approach is extremely powerful for investigating PPIs in situations where the labeling with fluorophores of the two interacting partners is possible.

For FRET to occur - critical conditions on the distance between two fluorophores are required[8,9]. The two fluorophores should not be distant from each other by more than 10 nm. Therefore, cautions must be taken when designing FLIM-FRET experiments to ensure that the donor and the acceptor of fluorescence have a chance to be located close to each other in the interacting complex. While this may seem constraining, it is in fact a true advantage as the distance-dependence of FRET ensures that two labelled proteins undergoing FRET have to physically interact (**Figure 1A**). The difficulties at getting clear answers about PPI in colocalization

experiments (two colocalized proteins may not necessarily interact) are therefore not an issue using FLIM-FRET.

[Place Figure 1 here]

A second requirement for FRET is that the emission spectrum of the donor and the absorption spectra of the acceptor should overlap[8] (**Figure 1B**). The fluorescence excitation of the donor should be at wavelengths that contribute very little to the direct fluorescence excitation of the acceptor. Not all combinations of fluorophores are possible and we additionally recommend to preferentially use donors with monoexponential fluorescence decays to facilitate FLIM-FRET interpretations[10]. Several couples of fluorescence proteins meet these requirements, including the popular eGFP-mCherry couple[11] (for a review on the palette of available fluorescent protein FRET pairs see[12,13]).

FLIM-FRET allows measuring the fluorescence lifetime decay of a FRET donor at every pixel of a FLIM image (**Figure 1A**). There are two major techniques to determine fluorescence lifetime that differ in acquisition and analysis: frequency-domain (FD)[14] and time-domain (TD). TD FLIM is more widespread and is performed using a pulsed illumination combined with different possible detection configurations including gating methods[15], streak camera[16] or time-correlated single photon counting (TCSPC) techniques[8]. For both FD and TD techniques, fluorescence lifetime is not directly measured but requires an analysis of the measured data to estimate the lifetime(s) or the presence of interactions. For TCSPC techniques, the most widely used analysis relies on fitting the decays with single or multi exponential functions using least square iterative re-convolutions that minimize the weighted sum of the residuals.

Finally, FLIM-FRET can be performed both by using single photon or multiphoton excitations. The latest have several advantages like reducing autofluorescence and photodamage out of the focal plane. Multiphoton excitations allow also a longer excitation depth if working in thick 3D samples[8]. On the contrary, single photon excitation is usually more efficient as the two-photon absorption cross sections of fluorescent proteins are limited[17].

Here, we propose a protocol for FLIM-FRET measurements of PPIs in live *P. aeruginosa* in the particular case of two interacting proteins (PvdA and PvdL) expressed with highly different numbers of copies to demonstrate the quality and robustness of the technique at revealing critical features of PPIs. PvdA and PvdL proteins are involved in pyoverdine biosynthesis. PvdA is a L-ornithine N5-oxygenase and synthesizes the L-N5-formyl-N5-hydroxyornithine from L-ornithine by hydroxylation (PvdA) and formylation (PvdF)[18]. PvdL is a non-ribosomal peptide synthesis (NRPS) enzyme composed of four modules. The first module catalyzes the acylation of myristic acid. The second module catalyzes the activation of L-Glu and its condensation to the myristic-coA. Then, the third module condenses a L-Tyr amino acid that is then isomerized in D-Tyr. Finally, the fourth module binds a L-Dab (Diaminobutyric acid) amino acid to form the acylated tripeptide L-Glu/D-Tyr/L-Dab[6]. PvdL is thus responsible for the synthesis of the three first amino acids of the pyoverdine precursor. The interaction of PvdA protein with PvdL is surprising as PvdL, on the contrary to PvdI and PvdJ, does not carry a module specific for the L-

N5-formyl-N5-hydroxyornithine. This interaction suggest that all the enzymes responsible for the pyoverdine precursor biosynthesis are arranged in large transient and dynamic multi-enzymatic complexes[19,20].

In this report we explain in detail how to construct the bacterial strains expressing natively the two interacting eGFP and mCherry labelled proteins. We also describe sample preparation and conditions for efficient FLIM-FRET cell imaging. Finally, we propose a step-by-step tutorial for image analysis including a recently developed tool providing advanced visualization possibilities for straightforward interpretation of complex FLIM-FRET data. With this report, we would like to convince not only adventurous but most biologists that FRET-FLIM is an accessible and powerful technique able to address their questions about PPIs directly in the native cellular environment.

PROTOCOL:

1. Plasmid construction

1.1 Amplify by two PCR (PCR1 and 3) the DNA sequences (use genomic DNA of *P. aeruginosa* PAO1) of the 700 base pairs upstream and downstream of the regions corresponding to the insertion site in *P. aeruginosa* genome with high-fidelity DNA polymerase. Add restriction sites to primers in blue and green and add an overlapping sequence with mCherry to primers in red (**Figure 2**).

1.1.1 For PvdA labelled at the C-terminus with eGFP, amplify the 700 bp region upstream relative to the stop codon by the primers in blue, and amplify the 700 bp downstream region containing the stop codon with the primers in green.

1.1.2 For PvdL labelled at the N-terminus with mCherry, amplify the 700 bp region upstream to the PvdL gene, including the start codon, by the primers in blue, and amplify the 700 bp downstream region with the primers in green.

[Place Figure 2 here]

1.2 Amplify the eGFP encoding DNA (without the start and stop codons) with primers in red with High-Fidelity DNA polymerase.

1.3 Purify the PCR products on a PCR clean up column (**Table of Materials**).

1.4 Mix overlapping PCR products in equimolar ratio and perform a second PCR using primers with restriction site used for PCR 1 and 3 (green and blue in **Figure 2**).

1.5 Migrate the PCR product in agarose-1x TAE (Tris-Base Acetate EDTA pH 8.0) gel, cut the corresponding band and extract the amplicon with a PCR clean up kit (**Table of Materials**).

NOTE: The protocol can be paused here.

1.6 Digest PCR amplicon and pEXG2 plasmid using the corresponding restriction enzymes[21].

1.7 Ligate plasmid and insert with T4 DNA ligase using 90 ng of plasmid and molecular ratio 1:1 (plasmid:insert).

1.8 Transform plasmids construction in chemically competent cells *E. coli* TOP10 cells by mixing ligation product and 100 µL of TOP10. Incubate the competent bacteria/plasmid mixture on ice for 30 min before proceeding with a 42 °C heat shock for 60 s. Then, put the tube on ice for 10 min.

1.9 Add 1 mL of lysogeny broth (LB) to the bacteria and incubate at 37 °C for 1 h.

1.10 Plate 100 µL bacteria on LB agar containing 15 µg/mL gentamicin.

1.11 Incubate overnight at 37 °C.

1.12 Screen the presence of the insert by colony PCR: from one isolated transformant colony, pick up a minute amount of bacteria to be added to a PCR mix containing primers hybridizing on the plasmid in such a way that the presence of the amplicon could be detected by running the product on an agarose gel (DNA polymerase). From the same colony used for PCR, transfer a small amount of bacteria on a fresh plate containing 15 µg/mL gentamicin to be isolated and used for plasmid extraction. Finally, isolate and purify the plasmid (**Table of Materials**) and verify the insert by sequencing.

1.13 Store TOP10 bacteria containing the plasmid in LB with 20 % glycerol in 1.5 mL microtube at -80 °C and the purified plasmid at -20 °C in 1.5 mL tube.

NOTE: The protocol can be paused here

2 Fluorescent tag insertion into the chromosomal genome of P. aeruginosa (Figure 3)

2.1 Grow *P. aeruginosa*, TOP10 and *E. coli* helper bacteria, each one in 5 mL of LB without antibiotic at 30 °C under orbital shaking overnight[22]. Generate fluorescent tag insertion in the genome of *P. aeruginosa* by transferring the plasmid from E. coli TOP10 into the PAO1 strain and integrating the plasmid into the genome by homologous recombination. A second crossing-over event excising the vector generate the corresponding mutant.

2.2 Measure the optical density at 600 nm ($OD_{600\ nm}$) of the bacterial culture and mix an equal quantity of *P. aeruginosa* (500 µL, $OD_{600\ nm}$ = 1.0) with *E. coli* TOP10 pEXG2 (500 µL, $OD_{600\ nm}$ = 1.0) and *E. coli* HB101 pRK600 helper (500 µL, $OD_{600\ nm}$ = 1.0) in 1.5 mL microtube.

2.3 Centrifuge 5 min at 9,300 x *g* to pellet the bacteria.

NOTE: Online tools can be used to convert centrifugal g-force to rotation per minute (rpm) to adjust the centrifuge speed.

2.4 Keep the bacterial pellet and discard the supernatant.

2.5 Resuspend the pellet containing bacteria in 50 µL of LB.

2.6 Plate a spot (~50 µL) of the mixture on the middle of LB agar (preheat at 37 °C) and incubate 5 h at 37 °C.

2.7 Scrap the spot with a sterile inoculation loop and resuspend in 1 mL of LB.

2.8 Plate 100 µL of this bacterial suspension on LB agar containing 10 µg/mL chloramphenicol to eliminate *E. coli* (*E. coli* TOP10 pEXG2 and *E. coli* HB101 pRK600 helper are sensitive to chloramphenicol but *P. aeruginosa* is naturally resistant) and 30 µg/mL gentamicin and incubate 2 days at 37 °C.

2.9 Resuspend one colony in 1 mL LB and incubate at 37 °C under orbital shaking 4h.

2.10 Centrifuge 3 min at 9,300 x *g* and discard 950 µL of supernatant. Resuspend the pellet in 50 µL of LB and isolate the mixture on LB agar containing sucrose and without NaCl.

2.11 Incubate overnight at 30 °C.

2.12 Spot isolated colonies on LB agar and LB agar containing 15 mg/mL gentamicin in order to check the gentamicin sensitivity.

2.13 Verify the eGFP or mCherry insertion by PCR colonies (DNA polymerase) and sequencing using specific primers.

[Place Figure 3 here]

3 Pyoverdine measurement

3.1 Grow bacteria in 5 mL of LB at 30 °C under orbital shaking overnight.

3.2 Pellet bacteria by centrifugation, wash and grow them in 5 mL of SM (Succinate Medium, composition: 6 $g \cdot L^{-1}$ K_2HPO_4, 3 $g \cdot L^{-1}$ KH_2PO_4, 1 $g \cdot L^{-1}$ $(NH_4)_2$ SO_4, 0.2 $g \cdot L^{-1}$ $MgSO_4$, 7 H_2O and 4 $g \cdot L^{-1}$ sodium succinate with the pH adjusted to 7.0 by adding NaOH) at 30 °C under orbital shaking overnight. SM is an iron-deprived medium - the absence of iron will activate the expression of the proteins of the pyoverdine pathway normally repressed in the presence of iron.

3.3 Measure $OD_{600\,nm}$ and dilute bacteria again in fresh SM medium at $OD_{600\,nm}$ = 0.1 and grow them at 30 °C under orbital shaking overnight.

3.4 Measure $OD_{600\ nm}$ to determine the quantity of bacteria in each sample.

3.5 Prepare a quartz cuvette containing 100 µL of *P. aeruginosa* culture and complete to 1 mL of SM (900 µL). Prepare a quartz cuvette containing 1 mL of SM medium (blank).

3.6 Using a UV-visible spectrophotometer, measure the absorbance at the maximum of the absorption peak. At pH 7.0, the maximum of absorption of pyoverdine will occur at ~400 nm. Determine the pyoverdine (apo form) concentration in sample using the Beer-Lambert law using a molar extinction coefficient at 400 nm of ε = 19 000 $M^{-1} \cdot cm^{-1}$.

NOTE: Pyoverdine can be quantified in the range of absorbance from ~0.1 to ~1 (depending on UV-Visible spectrophotometer) in which the absorbance linearly increases with concentration.

4 Bacteria culture and conditions for cells to express PvdA, PvdL and PvdJ

4.1 On day 1, inoculate a tube with 5 mL of LB from the appropriate glycerol stock of bacteria and grow bacteria over night at 30 °C at 200 rpm in an orbital shaker incubator.

4.2 On day 2, pellet cells by centrifugation at 3,000 x *g* for 3 min and discard the supernatant.

4.3 Resuspend the cells in 10 mL of SM.

4.4 Repeat steps 4.2-4.3 once and grow bacteria in SM overnight at 30 °C 200 rpm.

4.5 On day 3, dilute 1/10 the bacteria culture in fresh SM.

4.6 Grow diluted bacteria again overnight at the same conditions.

NOTE: The presence of pyoverdine can be detected visually as it colors in yellow-green the growing media. It shows that the expression of the proteins of the pyoverdine pathway have been activated and that enzymes of interest are being expressed in the cells.

5 Preparation of agarose pad (Figure 4)

5.1 Place a microscope glass-slide on a flat horizontal surface. Arrange two glass-slides topped with two layers of adhesive tape on each side of the initial slide.

NOTE: Keep a 1-2 mm space between the three aligned slides to prevent the meleted agarose to eventually spread on the slides with adhesive tape.

5.2 Pipette and pour a droplet of 70 µL of 1% melted agarose on the glass-slide. Add a fourth slide on the top to flatten the agarose droplet and press down gently. Wait about a minute.

5.3 Take off the upper slide and drop with a pipette about 3 µL of bacteria into 3 to 4 spots at different locations onto the agarose pad.

5.4 Cover with a microscopy glass coverslip (for example a 22x22 mm #1.5 thickness).

NOTE: Flatness and thickness of the coverslips are important for working with two-photon excitations. Precision coverslips with controlled uniform flatness and low autofluorescence are usually a good choice.

5.5 Fix the coverslip with melted paraffin to seal the coverslip onto the glass slide. Start by fixing the four corners of the coverslip.

[Place Figure 4 here]

6 Imaging with a two-photon microscopy setup

NOTE: We are using a home-made two-photon excitation scanning inverted microscope with a 60x 1.2NA water immersion objective operating in de-scanned fluorescence collection mode. Two-photon excitation wavelength is set at 930 nm. It is provided by a Ti:Sapphire laser (80 MHz repetition rate, ≈ 70 fs pulse width) working at 10-20 mW. Fluorescence photons were collected through a 680 nm short pass filter and a 525/50 nm band-pass filter before being directed to a fiber-coupled avalanche photo-diode connected to a time-correlated single photon counting (TCSPC) module. The microscope is also equipped with a transmission fluorescence lamp. Several FLIM-FRET microscopes are now commercially available and many imaging facilities are equipped with setups able to perform FLIM-FRET measurements.

6.1 Use the fluorescence lamp to focus the objective on the monolayer of bacteria in the sample and select regions of interest.

6.2 Check that the excitation laser shutter is closed and that the infrared light coming from the laser is blocked and do not enter the microscope.

Caution: Careful attention and constant vigilance should be given working with IR pulsed lasers as the laser light cannot be seen by eyes but any and even transient direct exposition or laser reflection can be extremely harmful and create irreversible eye damages. Please refer to the local laser safety procedures and training before using microscopy setups.

6.3 Place the microscopy slide on the stage with the coverslips facing the objective.

6.4 Check that the fluorescence lamp is ON.

6.5 Turn the filter cube turret to select the eGFP cube and open the fluorescence lamp shutter.

6.6 Send the fluorescence light towards the eyepiece of the microscope.

Caution: Ensure appropriate filters are disposed in the light path to discard direct excitation light coming from the fluorescence lamp that can damage eyes.

6.7 Focus the objective on bacteria using the microscope knob.

6.8 Select a region of interest in the sample by translating it using the joystick controlling the motorized stage

NOTE: Focusing is easier with highly fluorescent sample allowing the fluorescence to be seen directly with eyes.

6.9 Switch the excitation for the 2PE laser for FLIM-FRET measurements.

6.10 Send the fluorescence emission path back towards the detector.

6.11 Turn back the filter cube turret to select for the dichroic cube for the 930 nm laser.

6.12 Set the laser power to 20 mW.

6.13 Set the size of the region of interest to 30 µm. This operation adjusts the voltage operating the galvo-mirrors and defines the range of their movements (**Figure 5**).

6.14 Turn on detector and start scanning the sample - the start and stop buttons controlling the scanning also control the opening and closing of the laser shutter both for safety reasons and to limit the photobleaching of the sample (**Figure 5**).

[Place Figure 5 here]

6.15 If necessary, adjust the focus by slightly moving the microscope fine focus knob.

6.16 Choose the field of view for imaging by moving finely the stage from the computer interface. This can be done on the setup by moving the cross on the image in the microscope control software (**Figure 5**) that will define the new center of the image and pressing **Move Stage**. A good field of view for acquisition corresponds to an image with 10-30 immobile bacteria, all correctly focused (all bacteria are on the same plane). If interested in extracting single cells FLIM-FRET data, ensure that bacteria are well individualized (image segmentation will be much easier).

6.17 Open the SPCM software (commercial software for data acquisition) and check that the photons count rate is not too high to avoid pile-up effect that can affect lifetime measurements. If necessary, lower down the laser intensity to keep the photon count rate low (around 1% of the laser repetition rate).

NOTE: Pile-Up effect describes the effects of photons lost at high photon count rates due to the dead time of the Time Correlated Single Photon Counting (TCSPC) devices. If Pile-Up occurs, the measured average lifetime becomes artificially shorter with possibly an additional shorter component that can appear in the decay due to the oversampling the fast-emitting photons.

6.18 Adjust acquisition parameters including the acquisition collection time (typically 60 s to 180 s are required to collect enough photons).

6.19 Press the **Start** button and wait for the acquisition to complete.

6.20 Save the data.

6.21 Stop scanning the sample and turn off the detector.

6.22 Select another field of view in sample and repeat steps 6.14-6.22 or image a new microscopy slide by repeating steps 6.1-6.22.

NOTE: *P. aeruginosa* can live and divide for up to 6-8 hours at room temperature on the agarose pad (corresponding to at last ~4 doubling time at 20°C). Ideally, do not wait too long to perform FLIM-FRET measurement to avoid observing a pad completely covered with bacteria.

7 Data analysis

7.1. Basic analysis

7.1.1 Run the SPCImage software.

7.1.2 Import the saved SPCM file. The intensity image is displayed on the left upper panel of the software (**Figure 6** blue box).

7.1.3 Examine the decay curve window (**Figure 6** green box) which displays the decay data corresponding to the pixel selected in the intensity image (**Figure 6** blue box). The photon numbers of each time channel are shown as blue dots and the fit of the decay is drawn as a red line. Note that after loading the data the software displays the brightest pixel of the image. Move the blue cross across the image to examine pixels with lower intensity. The decay window will automatically refresh at each new pixel position.

NOTE: Measuring the Instrumental Response Function (IRF) of a laser scanning system is very difficult. An IRF calculated from the rising edge of the fluorescence decay curves in the FLIM data can be used for decay deconvolution. This is the option done by default in SPCimage (**Figure 6** green curve).

[Place Figure 6 here]

7.1.4 Adjust the fitting range by moving the starting and ending channels of the fitting box (T1 and T2 in the green box). T1 should start at the first few channels of the rising decay and T2 define the last channel at the end of the decay and can be chosen as one of the last channels of the decay with a number of photons above the photons count offset (i.e., the levels of photons counted before the decay rises).

7.1.5 Choose the binning by changing the **Bin** value. The curve decay integrates the photon counting of the selected pixel together with an area of i pixels around the cursor position defined by the bin parameter (increasing the binning will increase the number of photons in the decay and may be helpful to reach the photon counts required for multi-exponential models).

7.1.6 Adjust the **Threshold** value. Pixels that do not have at least one channel with a number of photons higher than the threshold value will not be included in the fitting procedure. Of course the higher the number of pixels to fit, the longer the analysis.

NOTE: FLIM data can contain an enormous number of pixels and time channels. The last versions of the software allow using GPU (Graphics Processor Unit) to process a large number of pixels in parallel, which massively reduces processing times. It can be interesting to adjust the binning and threshold parameters using images corresponding to bacteria constructions exhibiting the lowest fluorescence intensity (e.g., with bacterial strains with the lowest expression levels). This will ensure that the relevant decays observed in these samples will meet the filtering criteria and will be included in the analysis. These parameters can then be used for all images.

7.1.7 Adjust, if necessary, the decay parameters (cyan box). Let the shift vary, most of the time scatter and offset can be fixed to zero if a look at the decay functions show that their contribution is negligible. The offset can be estimated looking at the first channels of the decay - note that imaging for a long time due to low fluorescence in the sample usually results in non-zero offset. Scattering occurs mostly in thick samples and can be considered negligible otherwise.

7.1.8 Before running the fit, select the fitting algorithm. Open the algorithm settings window in **Show/Hide Model Options**. Select maximum likelihood estimation (MLE) algorithm (**Figure 7A**).

[Place Figure 7 here]

7.1.9 Run the fitting of the image by clicking **Calculate | Decay matrix**. Once completed, the lifetime encoded FLIM image appears in the lifetime image panel (**Figure 6** purple box).

NOTE: On the decay curve window (**Figure 6** green box) it is possible to see the lifetime value that corresponds to each pixel of the image by moving the blue cross.

NOTE: to process a large number of similar FLIM data files automatically, a batch processing mode can be used.

7.1.10 Check the quality of the fit looking at the residuals (ideally distributed randomly around

0) and a Chi square value close to 1.

7.1.11 Fitted data can be exported in different formats. To export files in txt files, go to **File** | **Export**. In the **Export** options window (**Figure 7B**), choose **Select All** and then click **Export**.

7.1.12 Finally save the analysis file. Analysis files are saved as **.img* files and can be reopened directly in SPCImage.

NOTE: In particular cases of unbalanced donor/acceptor quantities, FLIM-FRET can reveal sub-populations in a mixture of interacting protein complexes - in particular when the concentrations of the two partners are very different, thus resulting in mixtures of complex and free species. Non-interacting species (characterized by a decay very similar to the donor only decay) can be discriminated from interacting ones assuming a spatial invariance of the donor lifetime components across the data set. Similarly, non-stoichiometric interacting complexes with either more donors or more acceptor of fluorescence may form. The fluorescence decays of such complexes are usually difficult to interpret. A FLIM diagram plot can be used to provide critical information about stoichiometry and binding mode of PPIs[20,23]. The FLIM diagram plot is a graphical representation of the shortest lifetime component as a function of its amplitude. It can be used to visualize pixels with similar decay signatures. To draw such representations, experimental fluorescence decays have to be fitted with a two exponential model. The following steps can be a guide through this process.

7.1.13 Start by analyzing the data of the donor only construction. It will allow determining the lifetime value of the donor. Ideally, measure this value over several images recorded in the same conditions as the donor/acceptor constructions to retrieve a robust lifetime value for the donor.

7.1.14 Once determined, fit the fluorescence decays of donor/acceptor constructions with a two-exponential model. In the cyan decay parameter box (**Figure 6**), set the number of components to 2. Fix t2(ps) parameter to the robust lifetime value of the donor determined in step 1 and check the box to fix this parameter.

NOTE: It is important to fix the long-lived lifetime τ2 in order to limit over-fitting, to improve fitting convergence, and to obtain more reliable two-exponential fit parameters[24,25,26].

7.1.15 Save the **img* file and export data as **.asc* files as in step 7.1.11.

7.2. Advanced analysis of the FLIM images in R

7.2.1 Install R (https://cran.r-project.org) and RStudio (https://rstudio.com) if necessary.

7.2.2 Open RStudio and create a new project.

7.2.3 Move all analysis **.asc* file in a folder called “data” in the project main folder.

7.2.4 Open a new script file (or open the supplementary script FLIM_analysis.R).

7.2.5 Install the dedicated flimDiagRam package for flim data analysis https://github.com/jgodet/flimDiagRam. Call the package in the workspace. (See the notice HowTo_FlimDiagRam)

NOTE: Installation of packages have to be done only once. Once installed, packages can be called from any new R session. Downloading R packages from github requires installing 'devtools' package. The installation of 'devtools' can take several minutes. The *flimDiagRam* package can be used to represent the parameters and distributions of the FLIM data, to extract FLIM data at the level of single individualized cells, to compare FLIM results across conditions or strains and to explore FLIM data using advanced visualization tools like the FLIM diagram plot.

7.2.6 Use the step-by-step commented code and the data are made available to independently reproduce all the sub-figures presented in the Representative Results section below. This tutorial can be found in the notice HowTo_FlimDiagRam at https://github.com/jgodet/flimDiagRam/blob/master/HowTo.pdf. The code can be easily transposed to analyze the data.

REPRESENTATIVE RESULTS:

Empirical cumulative distribution functions (ecdf) of the fluorescence lifetimes measured for the different bacterial strains are shown in **Figure 8**. If FRET occurs, the ecdfs are shifted towards the shorter-lived lifetimes (**Figure 8A,8B**). Note that when the interaction of the two proteins results in a long distance between the two fluorophores, no FRET can occur (**Figure 8C**). This situation cannot be distinguished from the absence of interaction between the two partners in FLIM. It is therefore important, when inter-dye distance cannot be predicted from molecular models or known architectures of the complex, to consider labelling the proteins at different positions to maximize chances to probe the interaction. Similarly, due to the large difference in protein expressions between PvdA (highly expressed) and the non-ribosomal peptide synthetase PvdL (few copies per cells), the same PvdA/PvdL complex does not result in similar FLIM-FRET data. In fact, unbalanced stoichiometries can complicate the interpretation of FLIM-FRET data. Depending on which protein is labelled with the donor, unbalanced stoichiometries lead to differences in the contribution of the free as compared to the bound donor-labelled proteins in the recorded fluorescence lifetime distribution (**Figure 8A,8B**).

[Place Figure 8 here]

The diagram plot can be used to provide critical information about the stoichiometry as seen in **Figure 9**. In the PvdA-eGFP/mCherry PvdL mutant, the quantity of donor-labelled PvdA is much higher than the quantity of mCherry PvdL. Amongst all donors present in the sample, only a few of them are interacting with PvdL. Contrary to the average FLIM value distribution, the FLIM diagram plot gives only the specific information contained in the decay component of the donors undergoing FRET. In **Figure 9A**, a single tau1 value centered at ~2.3 ns can be observed, representing about 30-40% of the species in the mixture. The single tau1 value suggests that each

PvdA-eGFP donor can only transfer with one mCherry PvdL acceptor.

From the reverse labelling (PvdA-mCherry/eGFP PvdL), most of the eGFP PvdL proteins are expected to interact with PvdA-mCherry, due to the low number of PvdL as compared to PvdA. This is confirmed by the alpha1 values that are shifted towards higher values. Moreover, the tau1 values became much more distributed (**Figure 9B**) with the apparition of short-lived species with lifetimes as low as ~1.5 ns. This suggests that additional transfers occur as compared to the situation in **Figure 9A** and thus, that multiple PvdA proteins may bind to a single PvdL protein. As a result, for each complex, the eGFP lifetime will depend on the number and distribution of mCherry proteins with which eGFP is transferring energy. Taken together, the data suggest that each PvdL protein can interact with multiple PvdA proteins

[Place Figure 9 here]

FIGURE AND TABLE LEGENDS:

Figure 1: FLIM-FRET analysis principle. Each pixel of the FLIM-FRET multidimensional image contains information about the fluorescence decay recorded at this particular location (#counts = number of detected photons in the channel t). (**A**) The classical representation of the FLIM image is usually a false-color lifetime encoded 2D image (left). A decrease in the mean fluorescence lifetime of the donor - as seen by a change in the color scale - can be observed in the presence of FRET and is informative about the presence of PPIs in this spatial area. (**B**) Overlap between the donor emission spectrum and the acceptor absorption spectrum is necessary for FRET to occur.

Figure 2: Overview of PCR strategy and plasmids construction used for the construction of PvdA-mCherry. See text for details - pvdA encodes an enzyme involved in the biosynthesis of the siderophore pyoverdine, a secondary metabolite involved in iron acquisition.

Figure 3: Protocol of construction of *P. aeruginosa* strains by fluorescent tag insertion. See text for details.

Figure 4: Agarose pad preparation.

Figure 5: Schematic representation of the interface of microscope control software.

Figure 6: Main panel of the data analysis window of SPCImage software. Intensity image (blue box), lifetime image (purple box), lifetime histogram (upper right), decay curve at selected position (green box), and decay parameters at selected position (cyan box) of a representative PvdA-eGFP decay recorded in live *P. aeruginosa* using a bh SPC830 acquisition card on a home-made Two-Photon Excitation-FLIM-FRET setup. The experimental decay curve of the pixel pointed in the above image, its mono-exponential fit (red curve) deconvoluting the decay from its calculated instrumental response function (green curve) can be seen in the green panel.

Figure 7: (A) Algorithm settings for fitting the decays with exponential models. Selecting MLE (maximum-likelihood algorithm or maximum-likelihood estimation, MLE) as the fit model, and **(B) export options window**.

Figure 8: Illustration of changes occurring in the donor mean fluorescence lifetime distribution in response to FRET (single exponential model). Representation of the interactions of PvdL (grey form) with PvdA (blue form) (**A and B**) or PvdJ (yellow form) (**C**) proteins labeled with eGFP (green) or mCherry (red) fluorescent proteins. The empirical cumulative distribution functions (lower graphs) can clearly highlight the differences between the fluorescence lifetime distributions. (**A**) In the presence of an excess of PvdA labeled with the donor of fluorescence, the mean lifetime distribution of eGFP donors is dominated by donors that do not undergo FRET but also integrate the lifetime of the few donors undergoing FRET with mCherry-PvdL. In this situation, the lifetime distribution of the mixture (green-orange curve) is close to the lifetime distribution of the same mixture formed with unlabeled PvdL only (green curve). (**B**) If the order of labelling is changed and an excess of PvdA labeled with acceptors is present, the mean lifetime distribution is governed by the transferring species, including possibly donors that undergo FRET with multiple acceptors (orange curve). This distribution is therefore very different from the same complex formed with unlabeled PvdA (green curve). (**C**) If no FRET occurs because proteins do not interact or because the inter-dye distance is too large in the complex, changes in the lifetime distribution is almost superimposable to that of the donor only (compare the light green curve corresponding to the fluorescence lifetime distribution of the PvdJ-eGFP/mCherry-PvdL to the green curve corresponding to PvdJ-eGFP).

Figure 9: FLIM diagram plots in case of excess of donors (A) or acceptors (B) and multiple binding sites. The FLIM diagram plot gives the specific information contained in the decay component of the donor undergoing FRET retrieved using a two-exponential fit. In the PvdA-eGFP/mCherry-PvdL mutant (**A**), a single tau1 value is observed and its amplitude given by the scattered position of the data points on the horizontal axis is informative about the population of donors engaged in FRET. In the PvdA-mCherry/eGFP-PvdL system (**B**), the tau1 values are much more distributed, indicating that one PvdL (grey form) protein may interact with multiple PvdA (blue form) proteins.

DISCUSSION:

FLIM-FRET offers some key advantages over intensity-based FRET imaging. Fluorescence lifetime is an intrinsic parameter of the fluorophore. As a consequence, it is not dependent on local concentrations of fluorophores neither on the intensity of the light excitation. The fluorescence lifetime is additionally also poorly affected by photo-bleaching. It is particularly interesting to evidence PPIs in cells where local proteins concentrations can be highly heterogeneous throughout the subcellular compartments or regions. FLIM-FRET is also interesting in all situations where the concentration of complex is low because the expression levels of both proteins or of one of the proteins are low.

In the context of PPIs, the FRET mechanisms responsible for the shortening of the lifetime and therefore information about the nature of the interactions are hard to infer considering only the

661 average lifetime. Indeed, a shortening of the average lifetime can be due to a high proportion of
662 species interacting with moderate FRET, or on the opposite to a low proportion of donors
663 interacting at a short distance with the acceptor. This situation is even more complicated when
664 complexes with unbalanced stoichiometries form. Graphical visualization tools allowing the
665 representation of several dimensions (in the case of the diagram plot tau1, alpha and <tau>) can
666 be useful to provide critical information on the nature of the complexes that form. Alternative
667 graphical representations of the data, like the phasor based analysis[27,28] proposing a graphical
668 representation of the raw FLIM data in a vector space, are also interesting in this context.
669
670 Choosing how to tag the proteins of interest is a key point for successful FLIM-FRET experiments.
671 Most critically, tags should not modify or alter the interaction of proteins. Unfortunately, except
672 in rare cases where the structures of the proteins are known or can be predicted, in most cases
673 one is compelled to trial-and-error approaches. Interpretations of FLIM-FRET in the absence of
674 energy transfer have therefore always to consider the possibility that labels can alter the
675 interaction. For this reason, FLIM-FRET can be seen as a confirmatory technique in the sense that
676 if an interaction is observed, it should exist in the absence of label. Disposing of an external
677 functional readout - like checking that the production of pyoverdine by the mutated strains
678 expressing doubly labelled proteins is similar to wild type strains - is particularly useful to
679 interpret FLIM-FRET results.
680
681 Imaging is not a high-throughput method for detecting PPIs and has been so far exploited to
682 confirm suspected or predicted PPIs. In this confirmatory context, pushing the analysis to extract
683 from the data as much information as possible makes sense to gain deeper understandings of
684 the mechanisms involved in the PPI. Some attempts are being performed[29,30,31] to turn FLIM-FRET
685 setups adapted to screening strategies. Developing advanced easily available and automated
686 analysis will ensure the possibility to process the large amount of data produced by high-
687 throughput screening methods. In this context, fitting procedures using least square methods
688 that require high count statistics might be poorly adapted to estimate FRET. A variety of
689 alternative methods have been developed[16,32], including non-fitting methods (reviewed in
690 Padilla-Parra et al. 2011 [33]). These methods differ in calculation speed, minimal number of
691 photons required for proper analysis, accuracy, complexity and type of data that can be
692 efficiently processed. Techniques like the minimal fraction of interacting donor[34] or phasor
693 approach[35,36,37] have the potential to perform high speed acquisitions in FRET–FLIM and still be
694 quantitative to process large amount of data or even to reach video-rate speeds.
695
696 The requirement of constructing fluorescently labelled protein that do not perturb the native
697 functions of the proteins in cells is a major concern for scaling up the speed and the number of
698 PPI explored. Alternative new labelling strategies, based for example on small-molecule
699 fluorogenic probes[38,39] may be a way to circumvent this critical limitation. Disposing of
700 fluorescent probes compatible with FLIM-FRET and able to label other cell components (like
701 nucleic acids or membrane) will also broaden the nature of the interactions FLIM-FRET can
702 characterize.
703

In a close future, we believe the greatest breakthrough in the FLIM-FRET field will result from innovation in data processing. Methods like compressed sensing[40] should enable efficient and accurate reconstruction of FLIM image from sparse decay data - possibly speeding up further the acquisition rate that would allow to perform real time FLIM-FRET on fast changing process. Similarly, machine learning applied to FLIM data regarding pixel classification or regression, denoising or signal restoration will allow outstanding image reconstruction and analysis that will further increase the interest of FRET-FLIM methods[41,42].

ACKNOWLEDGMENTS:

We acknowledge Dr Ludovic Richert for his valuable assistance on FLIM data acquisition and for the technical maintenance and development of the FLIM setup. This work was funded by grants from Fondation pour la Recherche en Chimie (https://icfrc.fr/). VN is funded by the Fondation pour la Recherche Médicale (FRM-SPF201809006906). YM is grateful to the Institut Universitaire de France (IUF) for support and providing additional time to be dedicated to research. IJS and JG acknowledge the Institute on Drug Delivery of Strasbourg for its financial support.

DISCLOSURES:

The authors have nothing to disclose.

REFERENCES:

1. Braun, P., Gingras, A. C. History of protein-protein interactions: From egg-white to complex networks. *Proteomics*. **12**, 1478–1498 (2012).
2. Nooren, I. M. A., Thornton, J. M. Structural characterisation and functional significance of transient protein-protein interactions. *Journal of Molecular Biology*. **325**, 991–1018 (2003).
3. Hayes, S., Malacrida, B., Kiely, M., Kiely, P. A. Studying protein-protein interactions: Progress, pitfalls and solutions. *Biochemical Society Transactions*. **44**, 994–1004 (2016).
4. Guillon, L., Altenburger, S., Graumann, P. L., Schalk, I. J. Deciphering protein dynamics of the siderophore pyoverdine pathway in Pseudomonas aeruginosa. *PLoS ONE* **8**, 1–9 (2013).
5. Ringel, M. T., Brüser, T. The biosynthesis of pyoverdines. *Microbial Cell*. **5**, 424–437 (2018).
6. Schalk, I. J., Rigouin, C., Godet, J. An overview of siderophore biosynthesis among fluorescent Pseudomonads and new insights into their complex cellular organization. *Environmental Microbiology*. **22**, 1447–1466 (2020).
7. Cui, Y. et al. Techniques for detecting protein-protein interactions in living cells: principles, limitations, and recent progress. *Science China Life Sciences*. (2019)
8. Day, R. N., Mazumder, N., Sun, Y., Christopher, K. G. FRET microscopy: Basics, issues and advantages of FLIM-FRET imaging. *Springer Series in Chemical Physics*. **111**, 249–276 (2015).
9. Bastiaens, P. I. H., Squire, A. Fluorescence lifetime imaging microscopy: Spatial resolution of biochemical processes in the cell. *Trends in Cell Biology*. **9**, 48–52 (1999).
10. Yasuda, R. Imaging spatiotemporal dynamics of neuronal signaling using fluorescence resonance energy transfer and fluorescence lifetime imaging microscopy. *Current Opinion in Neurobiology*. **16**, 551–561 (2006).
11. Tramier, M., Zahid, M., Mevel, J.-C., Masse, M.-J., Coppey-Moisan, M. Sensitivity of CFP/YFP and GFP/mCherry Pairs to Donor Photobleaching on FRET Determination by

748 Fluorescence Lifetime Imaging Microscopy in Living Cells. *Microscopy Research and Technique*.
749 **71**, 146–157 (2008).
750 12. Bajar, B. T., Wang, E. S., Zhang, S., Lin, M. Z., Chu, J. A guide to fluorescent protein FRET
751 pairs. *Sensors (Switzerland)* . **16**, 1–24 (2016).
752 13. Piston, D. W., Kremers, G. J. Fluorescent protein FRET: the good, the bad and the ugly.
753 *Trends in Biochemical Sciences*. **32**, 407–414 (2007).
754 14. Leray, A. et al. Optimized protocol of a frequency domain fluorescence lifetime imaging
755 microscope for fret measurements. *Microscopy Research and Technique*. **72**, 371–379 (2009).
756 15. Elson, D. S. et al. Real-time time-domain fluorescence lifetime imaging including single-
757 shot acquisition with a segmented optical image intensifier. *New Journal of Physics*. **6**, 1–13
758 (2004).
759 16. Rajoria, S., Zhao, L., Intes, X., Barroso, M. FLIM-FRET for Cancer Applications. *Current*
760 *Molecular Imaging.* **3**, 144–161 (2014).
761 17. Drobizhev, M., Makarov, N. S., Tillo, S. E., Hughes, T. E., Rebane, A. Two-photon
762 absorption properties of fluorescent proteins. *Nature Methods*. **8**, 393–399 (2011).
763 18. Visca, P., Ciervo, A., Orsi, N. Cloning and nucleotide sequence of the pvdA gene encoding
764 the pyoverdin biosynthetic enzyme L-ornithine N5-oxygenase in Pseudomonas aeruginosa.
765 *Journal of Bacteriology*. **176**, 1128–1140 (1994).
766 19. Imperi, F., Visca, P. Subcellular localization of the pyoverdine biogenesis machinery of
767 Pseudomonas aeruginosa: A membrane-associated 'siderosome'. *FEBS Letters*. **587**, 3387–3391
768 (2013).
769 20. Gasser, V. et al. In cellulo FRET-FLIM and single molecule tracking reveal the supra-
770 molecular organization of the pyoverdine bio-synthetic enzymes in Pseudomonas aeruginosa.
771 *Quarterly Reviews of Biophysics*. 1–11 (2019).
772 21. Rietsch, A., Mekalanos, J. J. Metabolic regulation of type III secretion gene expression in
773 Pseudomonas aeruginosa. *Molecular Microbiology*. **59**, 807–820 (2006).
774 22. Herrero, M., De Lorenzo, V., Timmis, K. N. Transposon vectors containing non-antibiotic
775 resistance selection markers for cloning and stable chromosomal insertion of foreign genes in
776 gram-negative bacteria. *Journal of Bacteriology*. **172**, 6557–6567 (1990).
777 23. Godet, J., Mély, Y. Exploring protein-protein interactions with large differences in protein
778 expression levels using FLIM-FRET. *Methods and Applications in Fluorescence*. **8**, 014007 (2019).
779 24. El Meshri, S. E. et al. Role of the nucleocapsid domain in HIV-1 gag oligomerization and
780 trafficking to the plasma membrane: A fluorescence lifetime imaging microscopy investigation.
781 *Journal of Molecular Biology*. **427**, 1480–1494 (2015).
782 25. Becker, W. The bh TCSPC Handbook. *Scanning*. 1–566 (2010).
783 26. Richert, L., Didier, P., de Rocquigny, H., Mély, Y. *Monitoring HIV-1 protein oligomerization*
784 *by FLIM FRET microscopy*. *Springer Series in Chemical Physics*. **111** (2015).
785 27. Fereidouni, F., Blab, G. A., Gerritsen, H. C. Phasor based analysis of FRET images recorded
786 using spectrally resolved lifetime imaging. *Methods and Applications in Fluorescence*. **2**, (2014).
787 28. Fereidouni, F., Gorpas, D., Ma, D., Fatakdawala, H., Marcu, L. Rapid fluorescence lifetime
788 estimation with modified phasor approach and Laguerre deconvolution: a comparative study.
789 *Methods and Applications in Fluorescence*. **5**, 035003 (2017).
790 29. Margineanu, A. et al. Screening for protein-protein interactions using Förster resonance
791 energy transfer (FRET) and fluorescence lifetime imaging microscopy (FLIM). *Scientific Reports*.

6, (2016).
30. Guzmán, C., Oetken-Lindholm, C., Abankwa, D. Automated High-Throughput Fluorescence Lifetime Imaging Microscopy to Detect Protein–Protein Interactions. *Journal of Laboratory Automation*. **21**, 238–245 (2016).
31. Liu, W., Cui, Y., Ren, W., Irudayaraj, J. Epigenetic biomarker screening by FLIM-FRET for combination therapy in ER+ breast cancer. *Clinical Epigenetics*. **11**, 1–9 (2019).
32. Liu, X. et al. Fast fluorescence lifetime imaging techniques: A review on challenge and development. *Journal of Innovative Optical Health Sciences*. **12**, 1–27 (2019).
33. Padilla-Parra, S., Auduge, N., Coppey-Moisan, M., Tramier, M. Non fitting based FRET-FLIM analysis approaches applied to quantify protein-protein interactions in live cells. *Biophysical Reviews*. **3**, 63–70 (2011).
34. Padilla-Parra, S., Audugé, N., Coppey-Moisan, M., Tramier, M. Quantitative FRET analysis by fast acquisition time domain FLIM at high spatial resolution in living cells. *Biophysical Journal*. **95**, 2976–2988 (2008).
35. Stringari, C. et al. Phasor approach to fluorescence lifetime microscopy distinguishes different metabolic states of germ cells in a live tissue. *Proceedings of the National Academy of Sciences of the United States of America*. **108**, 13582–13587 (2011).
36. Digman, M. A., Caiolfa, V. R., Zamai, M., Gratton, E. The phasor approach to fluorescence lifetime imaging analysis. *Biophysical Journal*. **94**, L14–L16 (2008).
37. Liang, Z., Lou, J., Scipioni, L., Gratton, E., Hinde, E. Quantifying nuclear wide chromatin compaction by phasor analysis of histone Förster resonance energy transfer (FRET) in frequency domain fluorescence lifetime imaging microscopy (FLIM) data. *Data in Brief*. **30**, 105401 (2020).
38. Grimm, J. B., Heckman, L. M., Lavis, L. D. *The chemistry of small-molecule fluorogenic probes*. *Progress in Molecular Biology and Translational Science*. **113** (Elsevier Inc., 2013).
39. Li, L., Sun, H. Next Generation of Small-Molecule Fluorogenic Probes for Bioimaging. *Biochemistry*. **59**, 216–217 (2020).
40. Yao, R., Ochoa, M., Yan, P., Intes, X. Net-FLICS: fast quantitative wide-field fluorescence lifetime imaging with compressed sensing – a deep learning approach. *Light: Science and Applications*. **8**, 1–7 (2019).
41. Smith, J. T. et al. Fast fit-free analysis of fluorescence lifetime imaging via deep learning. *Proceedings of the National Academy of Sciences of the United States of America*. **116**, 24019–24030 (2019).
42. Yao, R., Ochoa, M., Intes, X., Yan, P. Deep compressive macroscopic fluorescence lifetime imaging. *Proceedings - International Symposium on Biomedical Imaging*. **2018-April**, 908–911 (2018).

Figure 1

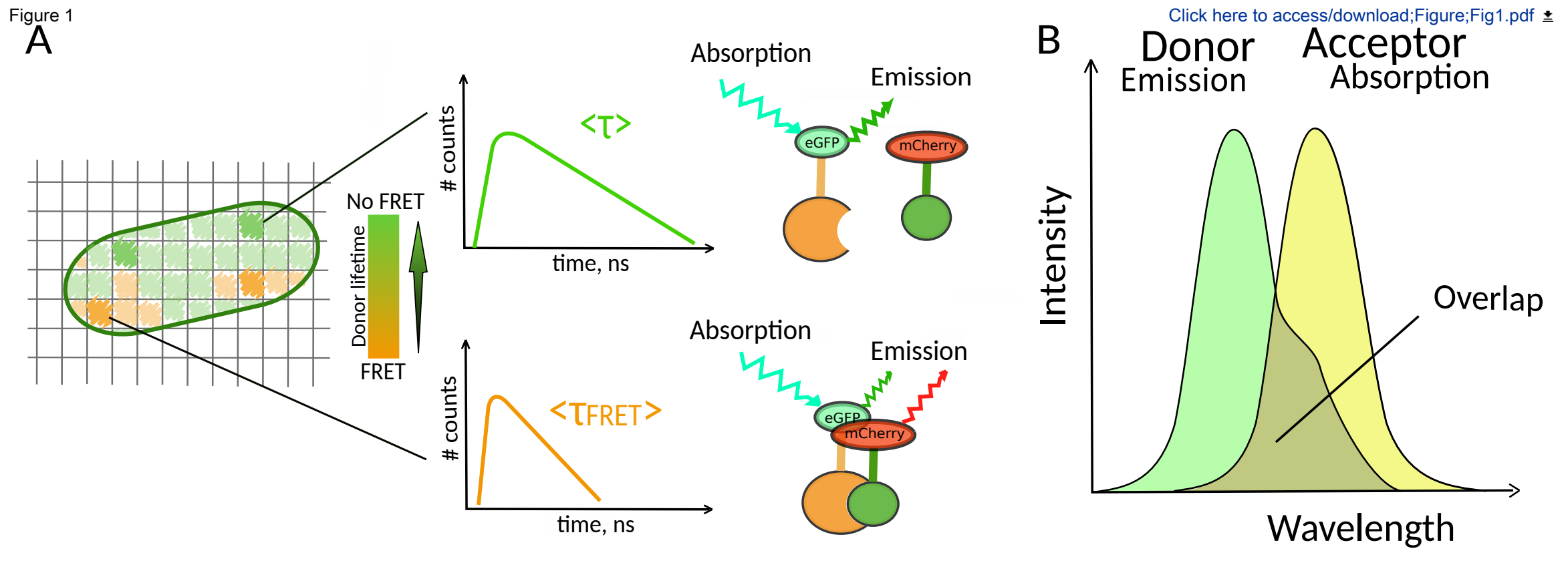

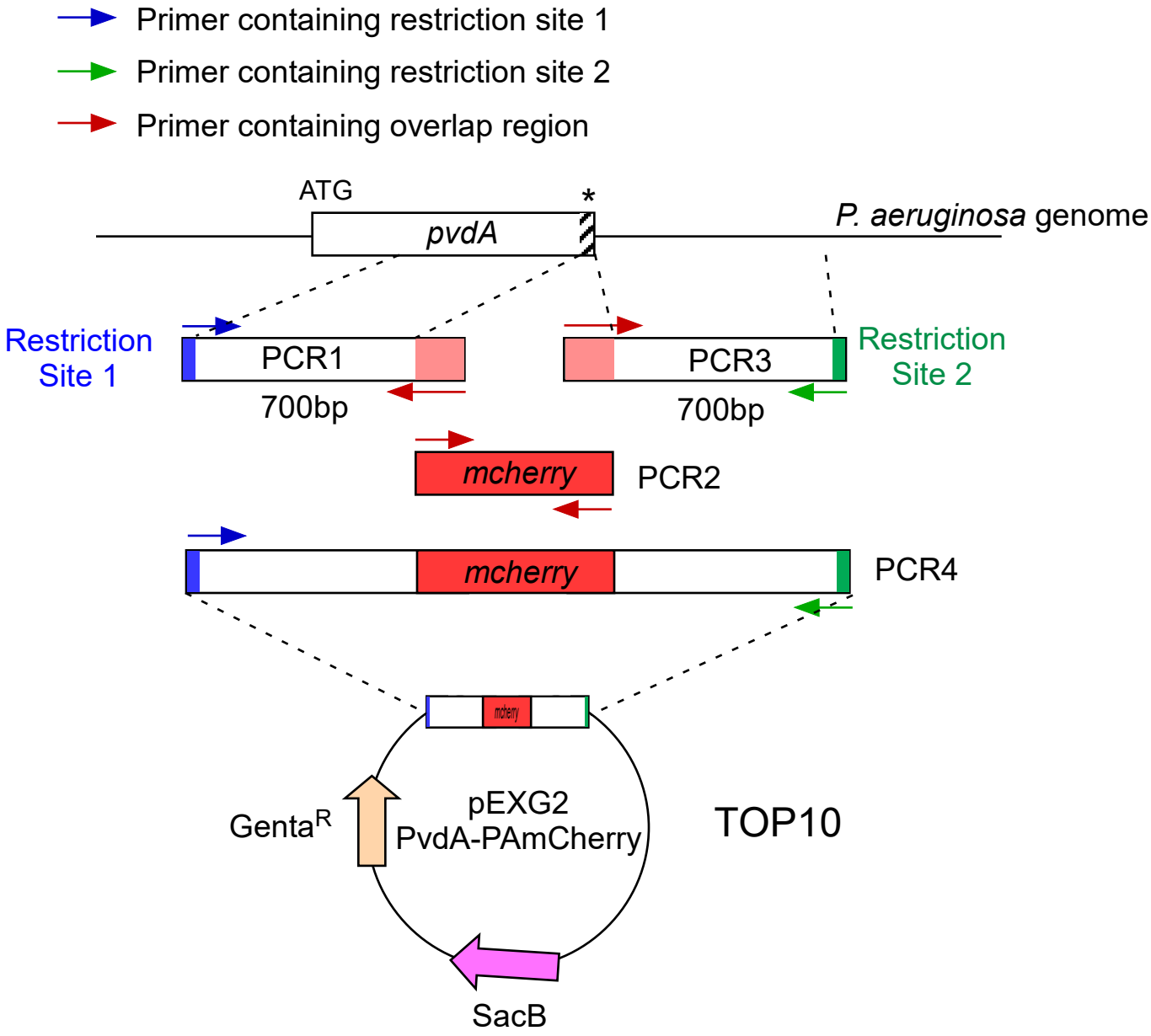

Figure 3

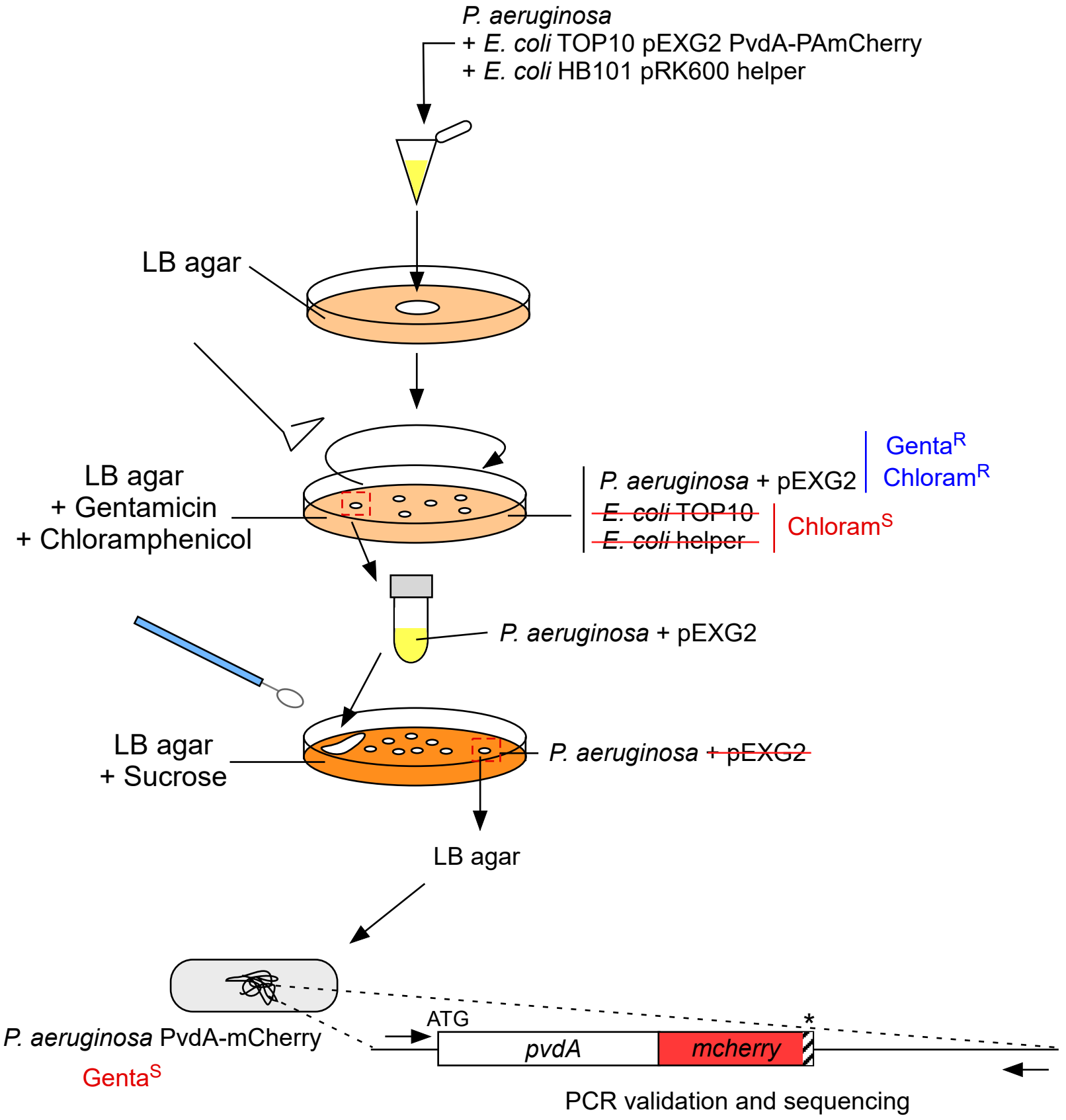

Figure 4

Click here to access/download;Figure;Fig4.pdf

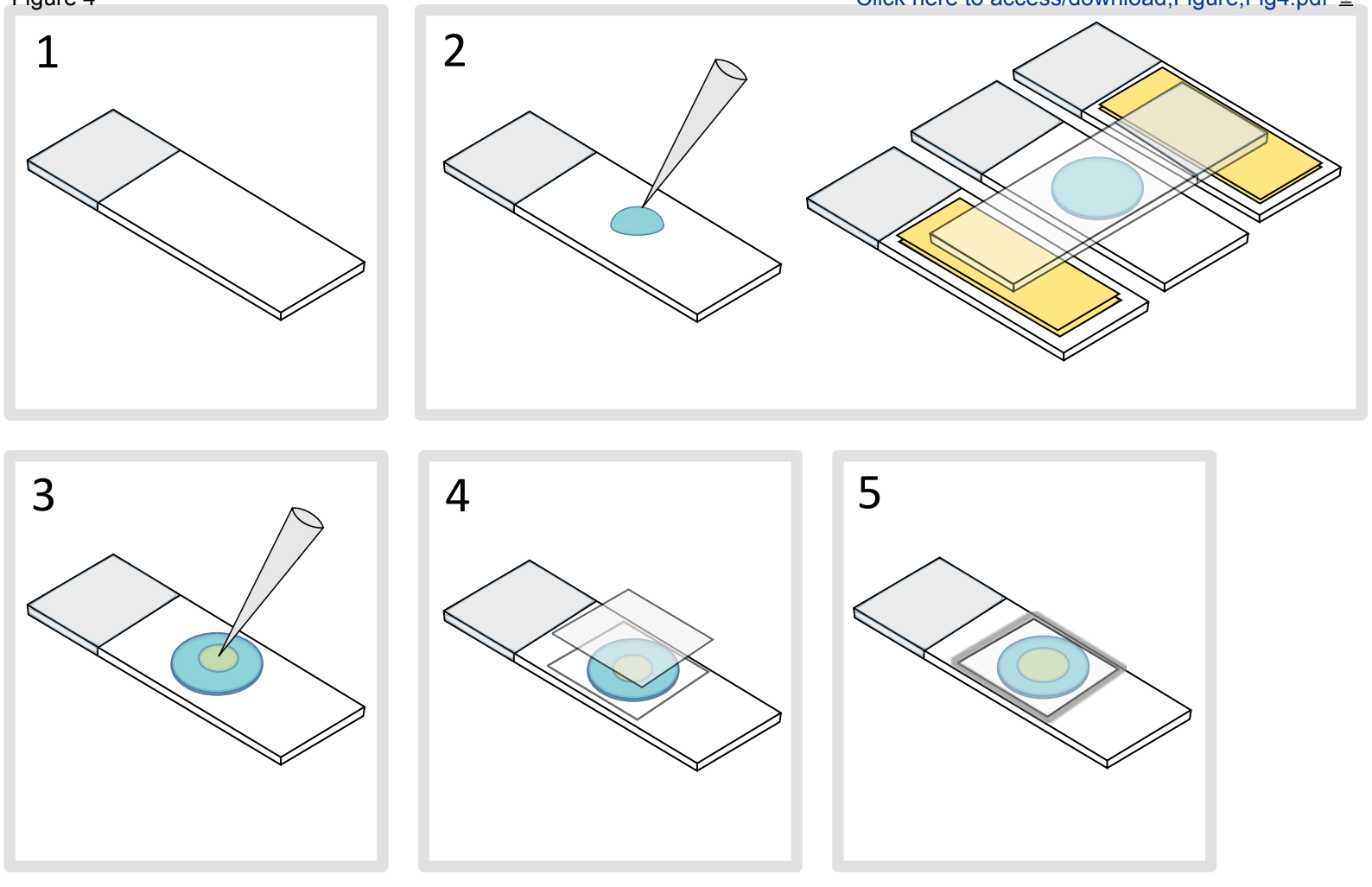

Figure 5

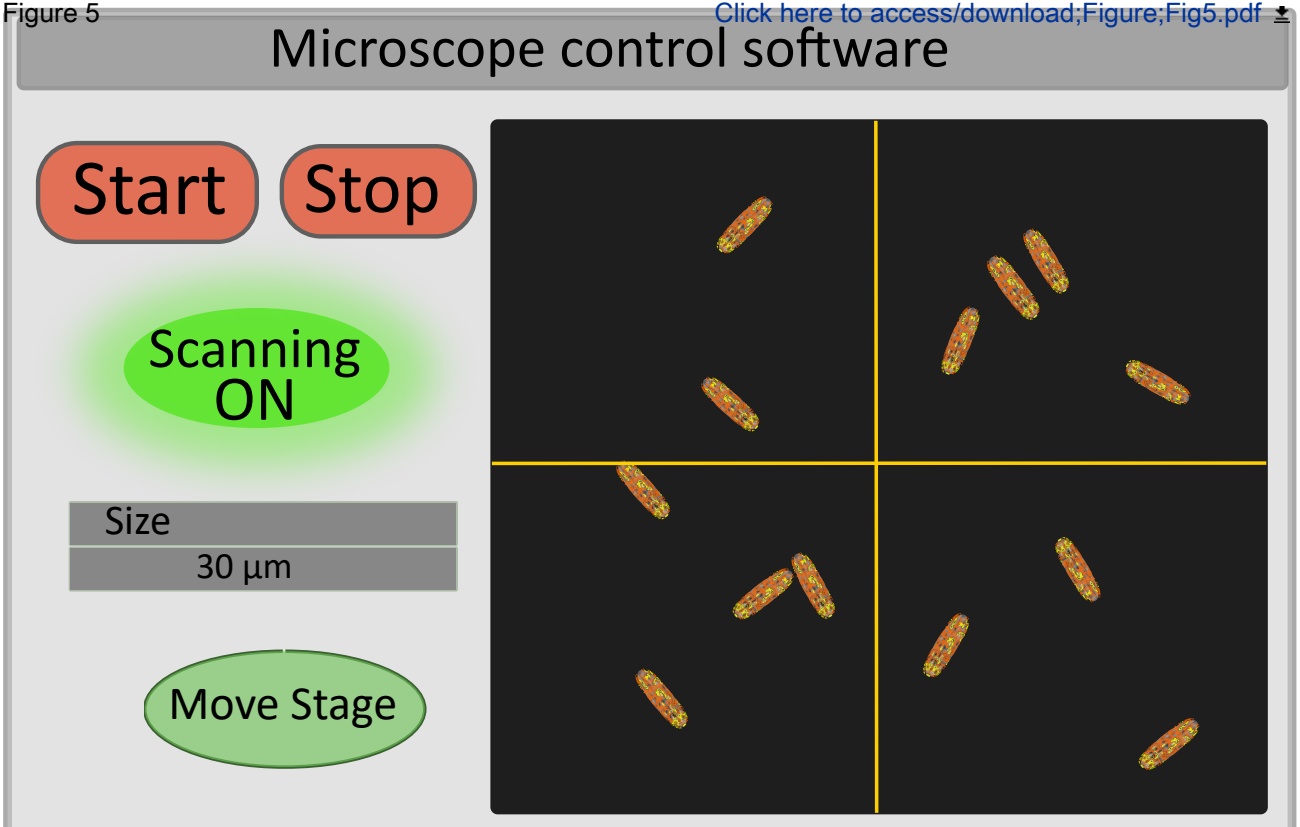

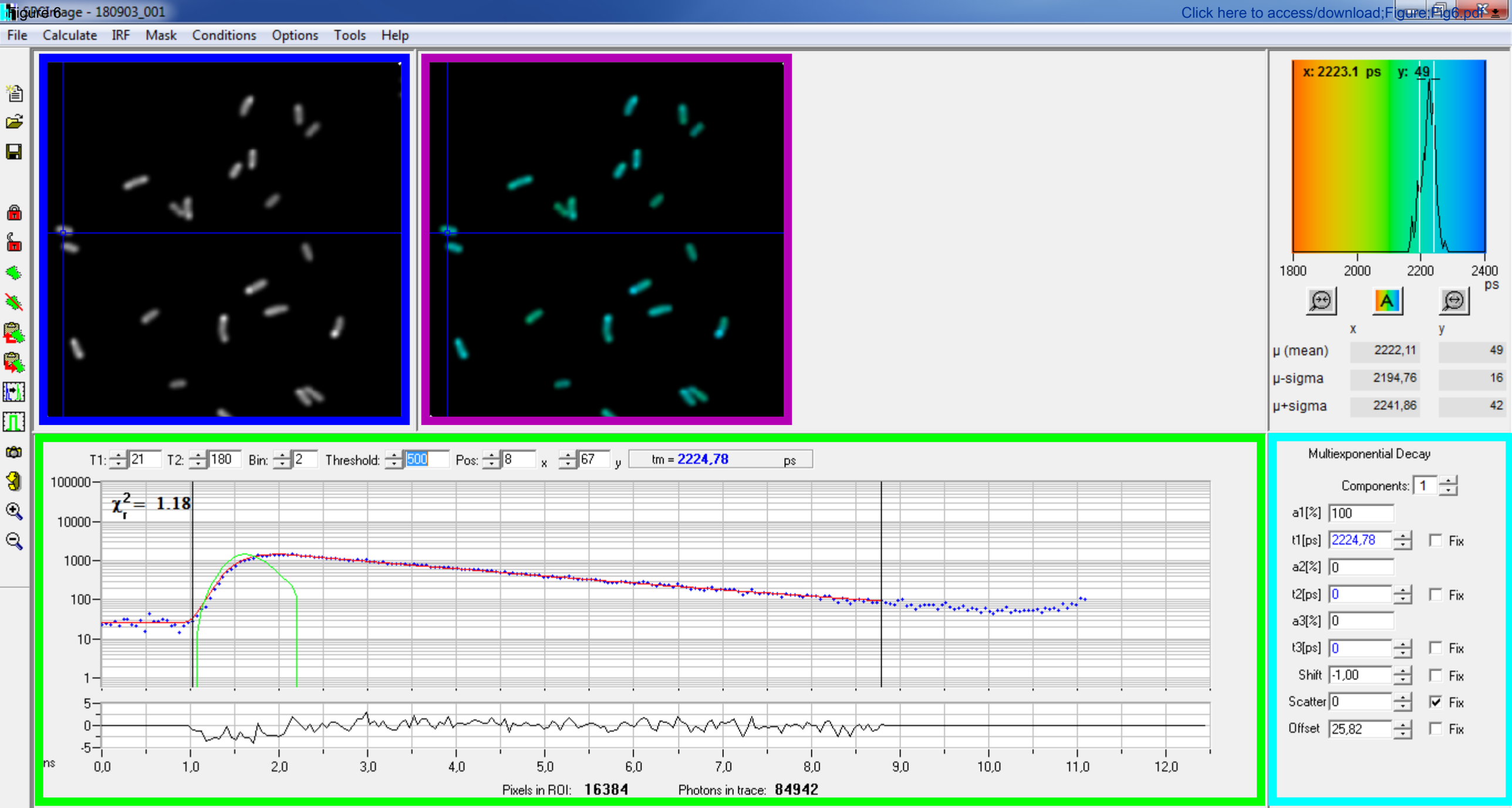

Figure 7

Click here to access/download;Figure;Fig7.pdf

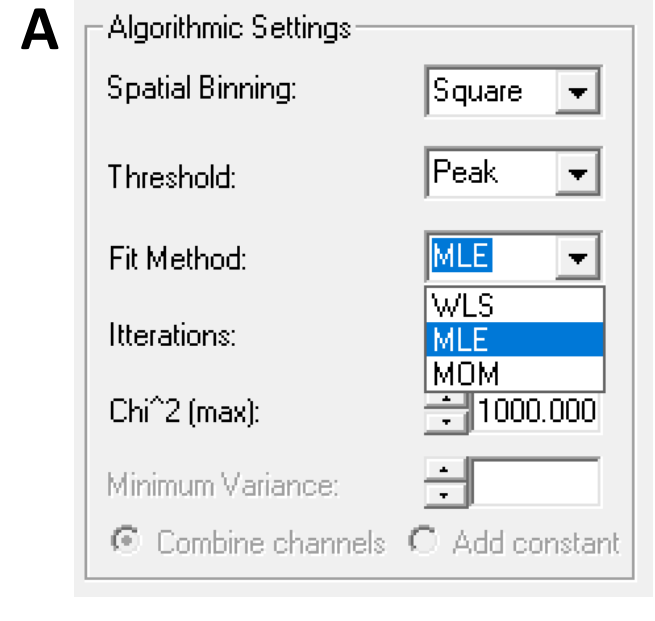

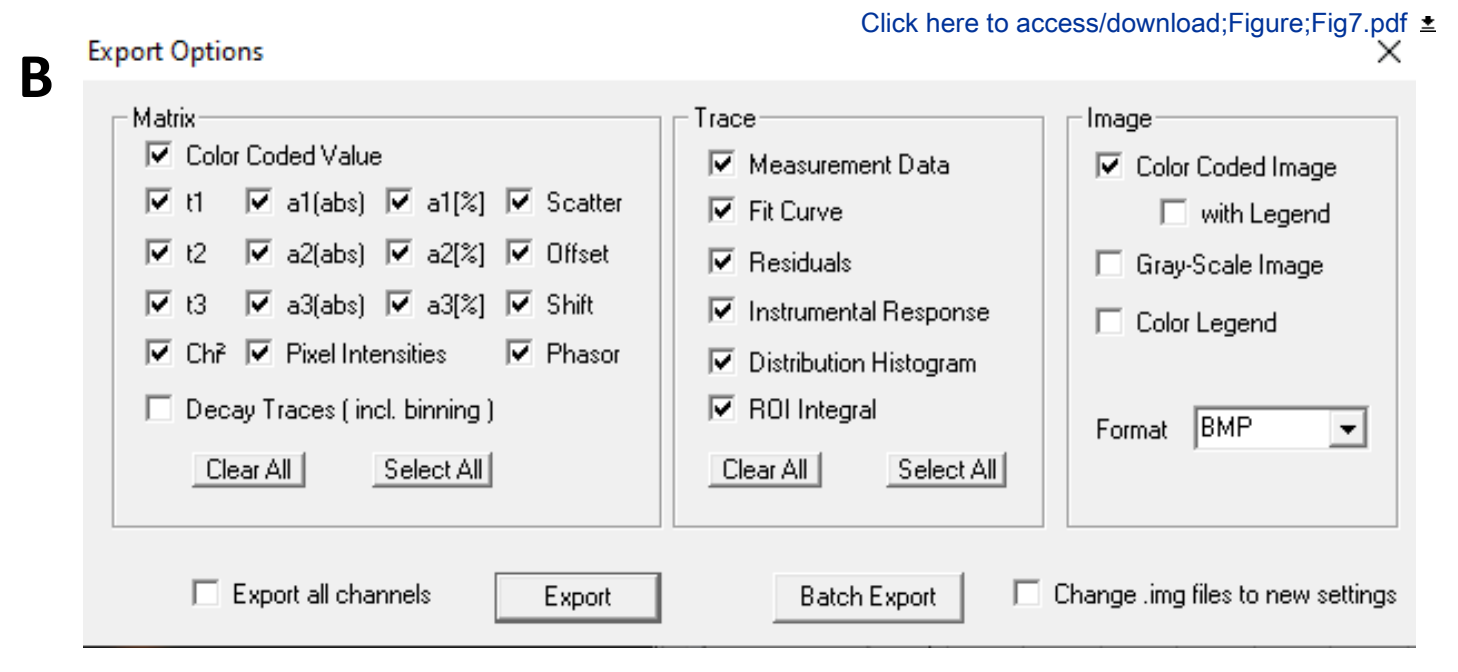

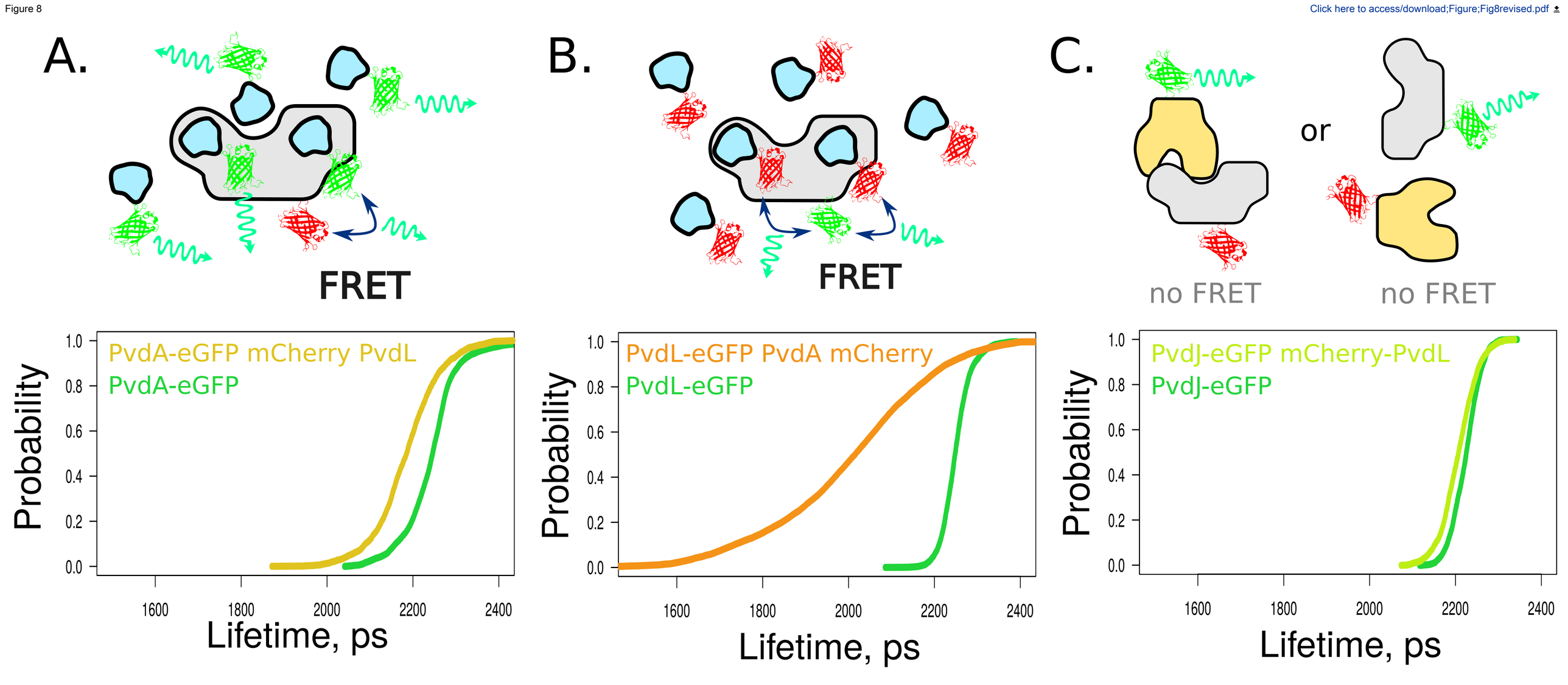

Figure 9

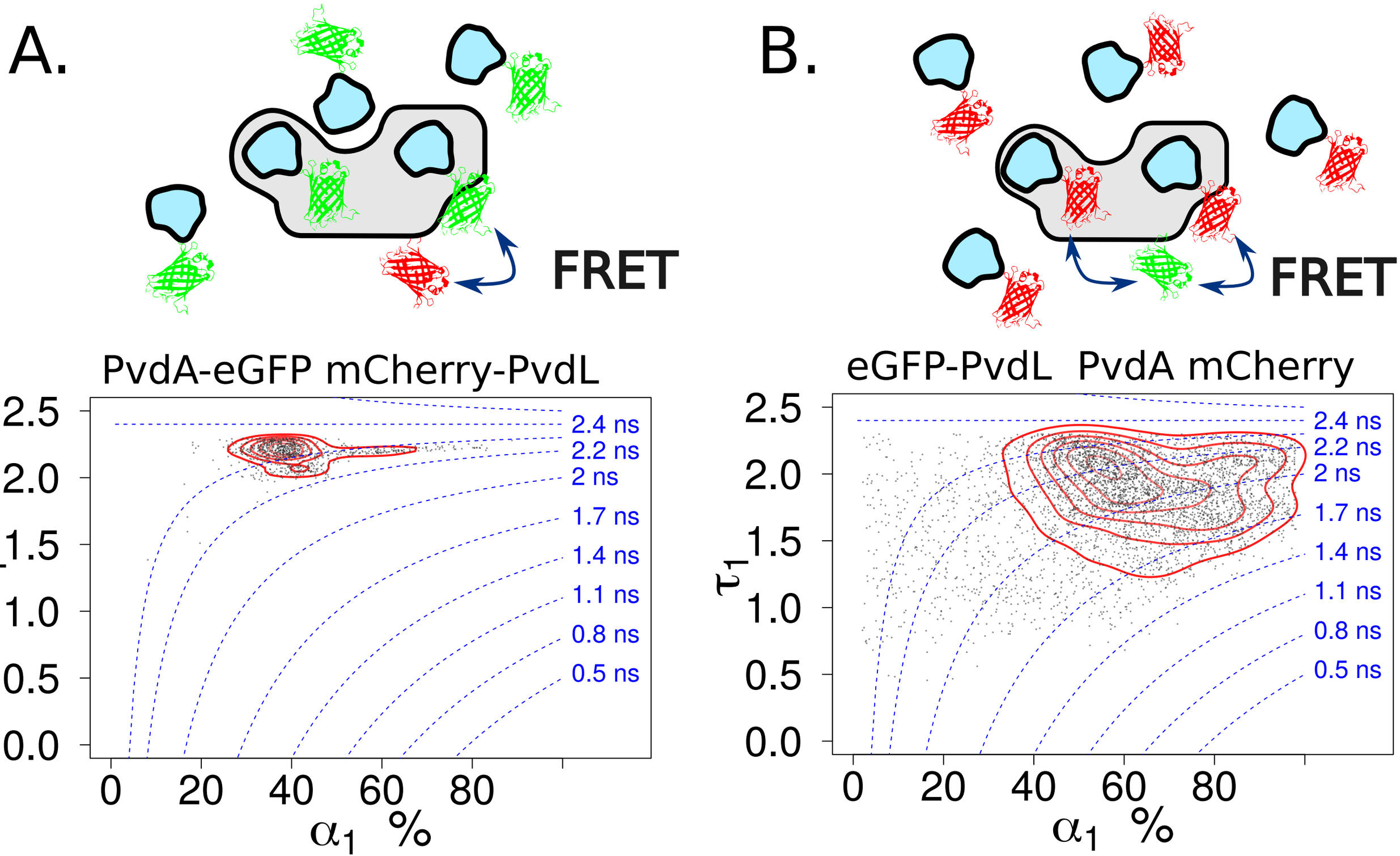

Table of Materials

Click here to access/download;Table of Materials;Table_of_Materials_revised.xlsx

Name of Material/Equipment	Company
525/50 nm band-pass filter	F37-516, AHF, Germany
680 nm short pass filter	F75-680, AHF, Germany
Agarose	Sigma-Aldrich
Ammonium Sulfate (NH4)2SO4	Sigma-Aldrich
DreamTaq DNA polymerase 5U/µL	ThermoFisher Scientific
E. coli TOP10	Invitrogen
Fiber-coupled avalanche photo-diode	SPCM-AQR-14- FC, Perkin Elmer
Glass coverslips (Thickness No. 1.5, 20×20mm	Knitel glass
High-Fidelity DNA polymerase Phusion 2U/µL	ThermoFisher Scientific
Lysogeny broth (LB)	Millipore
Magnesium Sulfate Heptahydrate (MgSO4 . 7H2O)	Sigma-Aldrich
Microscope slides (25×75mm)	Knitel glass
NucleoSpin Gel and PCR Clean-up	Macherey-Nagel
NucleoSpin Plasmid	Macherey-Nagel
Potassium Phosphate Dibasic (K2HPO4)	Sigma-Aldrich
Potassium Phosphate Monobasic (KH2PO4)	Sigma-Aldrich
Sodium Succinate (Disodium)	Sigma-Aldrich
SPCImage, SPCM software	Becker & Hickl
Sterile inoculating loop	Nunc
T4 DNA ligase 1U/µL	ThermoFisher Scientific
TCSPC module	SPC830, Becker & Hickl, Germany
Ti:Sapphire laser	Insight DeepSee, Spectra Physics
Tubes 50mL	Falcon

Catalog Number	Comments/Description
A9539	
A4418	
EP0714	
C404010	
MS0011	
F530S	
1.10285	
10034-99-8	
MS0057	
740609.50	
740588.10	
RES20765	
P5655	
14160	
7648-1PAK	
15224017	
352070	

We thank the Referees for their interest in our work and for helpful comments that will greatly improve the manuscript. We endeavored to respond to all the points raised. The Referees have brought up some good points and we appreciate the opportunity to improve our manuscript accordingly.

Reviewers' comments:
Reviewer #1:
Manuscript Summary:
Manko et al establish a clear protocol for the FRET-FLIM approach used in Gasser et al, although I found the protocol well developed, and the software used easy to install/use I have a few suggestions to help clarify and also not raise expectations too much for an unexperienced user.

Major Concerns:
One of the main points that are missed is that choosing how to tag PvdA and PvdL is an essential question. Indeed when PvdA is tagged with eGFP and PvdL with mCherry, the FRET-FLIM signal is really low compared to when PvdA is tagged with mCherry and PvdL with eGFP. Fig.8A and Fig.8C are almost undistinguishable. It would be necessary to make this a clear point and add not only the fitted curves, but all the data points to Fig.8, as in Fig.9. Clearly in the case of Fig.8A many of the pixels will fall in a place where the change in tau is not significant and this interaction is inconclusive.

Choosing how to tag the proteins of interest is indeed a key point for successful FLIM-FRET experiments. Most critically, tags should not modify or alter the interaction of proteins. Unfortunately, excepted in rare cases where the structure of the proteins are known or can be predicted, in most cases one is compelled to trial-and-error approaches. Interpretations of FLIM-FRET in the absence of energy transfer have therefore always to consider the possibility that labels can alter the interaction. For this reason, FLIM-FRET can be seen as a confirmatory technique in the sense that if an interaction is observed, it should exist in the absence of label. Disposing of an external functional readout - like checking that the production of pyoverdine by the mutated strains expressing doubly labelled proteins is similar to wt strains - is particularly useful to interpret FLIM-FRET results. (this paragraph has been added to the main manuscript in the discussion section)

If protein of interest are interacting in a 1-to-1 complex, labelling one or the other protein with eGFP - the donor - (and the other with the acceptor) should give concordant FRET signals. In our manuscript, we further demonstrate that non 1-to-1 interactions can also be characterized. In this case, changing the labelling from one protein to the other leads to very different FRET signals from almost no apparent FRET in the presence of excess of donor, to (high) FRET value with almost 100% of species interacting in the presence of an excess of acceptor. Empirical cumulative distribution functions of the average mean lifetime for one or the other labelling scheme illustrate these differences (significant changes of the distribution in the presence of an excess of acceptor - and tiny or hardly discernable changes in the presence of an excess of donor). Disposing of both labelling schemes is a key part of the exploration.

So for example I disagree with statement: line 589 "As a consequence, it is not dependent on local concentrations of fluorophores neither on the intensity of the light excitation." which contradicts the following paragraph.

There is likely a misunderstanding on this point. The whole context of the sentence was "Fluorescence lifetime is an intrinsic parameter of the fluorophore. As a consequence, it is not dependent on local concentrations of fluorophores neither on the intensity of the light excitation." The absence of dependence on concentration and light excitation was standing for fluorescence lifetime and not for FRET. If it is true that FRET depends on concentrations - and particularly in the context of complexes with unbalanced stoichiometries - the fluorescence lifetime (i.e. the mean by which to access to FRET values) does not.

Minor Concerns:

There are always newer versions of fluorescent proteins in use, they depend on each organism, are eGFP and mCherry the latest available in P.aeruginosa? Would be good to review.

Choosing the optimal FP FRET pairs is a complex and ever moving forward field and we thought it was out of the scope of this protocol. In the revised version of the manuscript, we propose the interested reader to refer to recent reviews about palette of available FP FRET pairs.

What is the green line in Figure 6?

The green line corresponds to the Instrumental Response Function. The IRF results mostly from the convolution of the response functions of the detector and of the laser pulse duration. As we are using two-photons with fs-pulses, the IRF is not measured but estimated from the data. (see *The bh TCSPC Handbook* cited in ref 25).

The sentence "The experimental decay curve of the pixel pointed in the above image, its fit (red curve) deconvoluting the decay from its calculated instrumental response function (green curve) can be seen in the green panel." has been added to the legend of figure 6

I would add in Figures 8 and 9 the names of the fusions PvdA, PvdJ and PvdL because they are referred to in the text and it would make the story easier to follow/

Done

What version of R is needed?

The package has been developed using R version 3.5.2 (December 2018). The package is compatible with any latest R versions (including the major update to the 4.0 version) and is also likely compatible with all versions ≥ 3.0.2 (although not tested) because it does not call or import any other package. A *Depends* section has been added to the package description file to indicate dependency on a particular version of R (>= 3.5)

Please on the HowTo document clarify that you are running all commands from R and no need to go/clone from github is needed.

The sentence “Note that there is no need to clone the repository from github to use the package. Instead the package can be installed from the github source repository directly in R. “ has been added.

line 119: "immobilized so that they do not move during the imaging acquisition time." please change to "immobilized during the imaging acquisition time."

This sentence has been removed following the remark of referee 2

line 581: "mCherry with which eGFP is transferring energy. " change to "mCherry proteins with which eGFP is transferring energy.

Done

line 630: "Similarly,machine learning applied to FLIM data in term of pixel classification or regression, denoising or signal restauration will make possible to achieve outstanding image reconstruction and analysis" replace with Similarly, machine learning applied to FLIM data regarding pixel classification or regression, denoising or signal restOration will allow outstanding image reconstruction and analysis"

The sentence has been changed for “Similarly, machine learning applied to FLIM data regarding pixel classification or regression, denoising or signal restoration will allow outstanding image reconstruction and analysis that will further increase the interest of FRET-FLIM methods”

Reviewer #2:

Manuscript Summary:

The manuscript of Manko et al. presents a very complete protocole of FLIM-FRET measurements in bacteria to reveal and caracterize PPI. All the protocol is well presented and the manuscript is wrtitten in a comprehensive manner. This protocol is definitely of high interest to be published in JOVE (and particularly with the video support). To improve this work I have few suggestions.

Major Concerns:

- Other FLIM methods than TCSPC are not cited in the introduction. there is no any information regarding the acquisition time, photon budget.

This point has been addressed by adding this paragraph in the introduction

« FLIM-FRET allows measuring the fluorescence lifetime decay of a FRET donor at every pixel of a FLIM image (Figure 1A). There are two major techniques to determine fluorescence lifetime which differ in acquisition and analysis: Frequency-domain (FD)[14] and Time-domain (TD). TD FLIM is more widespread and is performed using a pulsed illumination combined with different possible detection configurations including gating methods[15], streak camera[16] or Time-correlated single photon counting (TCSPC) techniques[8]. For both FD and TD techniques, fluorescence lifetime is not directly measured but requires an analysis of the measured data to estimate the lifetime(s) or the presence of interactions. For TCSPC techniques, the most widely used analysis relies on fitting the decays with single or multi exponential functions using least square iterative re-convolutions that minimize the weighted sum of the residuals. »

- In fact the introduction presents that FLIM is abble to study spatial location of PPI but there is no real use of image regarding the data analysis, particularly in fig8 and 9. This point has to be clarified. If yous sale spatial location in the introduction you have to show interesting results regarding this approach.

We do agree with this statement. Even if FLIM-FRET has the potential to extract spatial location of PPI, it can be exploited in situations where PPI are localized at fixed position in the cell. It is obviously not the case in our data where the interacting proteins are diffusing freely throughout the cytoplasm. To make the manuscript clearer, we removed the section about spatial characterization in the introduction part and added the following comment in the discussion part: " As FLIM measure fluorescence decays for every pixel of the image, it can additionally provide information about where the interactions take place in cells at the pixel resolution. But the space component of FLIM can be exploited only if the observed structures are sufficiently stable over the acquisition time."

- In term of data analysis, only fitting procedure with models seems to be used. I have two concerns:

(i) what means lifetime in fig8? do you use é expo model and mean lifetime calculaition? single expo model? this has to be clarified.

In figure 8, lifetime stands for the mean lifetime of a single exponential model. This value is calculated for every pixel with more photons that the defined threshold. The ecdf of the distribution of these values are then plotted. To make the legend of fig 8 more precise, we added the expression "(single exponential model)" at the end of the figure 8 title.

(ii) in the perspective, you mention new methods to analyze FLIM with AI. But you do not consider already available non-fiting approches with mean lifetme coming from the mean arrival time or phasor determination. this is missed in the introduction and in the perspective. Moreover, this is an important aspect when considering photon budget and acquisition time (see above).

We indeed missed to report the non-fitting approaches. In the revised version, we added the following paragraph in the discussion section "In this context, fitting procedures using least square methods that require high count statistics might be poorly adapted to estimate FRET. A variety of alternative methods have been developed [16,32], including non-fitting methods (reviewed in Padilla-Parra et al. 2011 [33]). These methods differ in calculation speed, minimal number of photons required for proper analysis, accuracy, complexity and type of data that can be efficiently processed. Techniques like the minimal fraction of interacting donor[34] or phasor approach[35,36,37] have the potential to perform high speed acquisitions in FRET–FLIM and still be quantitative to process large amount of data or even to reach video-rate speeds.

"

Minor Concerns:
Add more details regarding data analysis strategies and fitting methods in order to understand well the different models and the different values. Particularly you can include it in the figure legends (fig6, 8, 9)

Please see answer to the first question

Legends of figures 6,7, 8 and 9 have also been updated

Reviewer #3:

Manuscript Summary:

This protocol describes a method that combines the use of fluorescence lifetime imaging microscopy and Forster resonance energy transfer (FILM-FRET) to study protein-protein interactions. Within they include the steps to construct the bacterial strains, preparation of the culture slide and parameters for efficient FLIM-FRET cell imaging. They also go through the data analysis of images and describe batch analysis systems. The highlighted portions seem to match well to the goals of the protocol and all images include in the written portion are well constructed to compliment the protocol.

Minor Concerns:

A few grammatical issues but nothing major.

We read carefully the manuscript and corrected some grammatical errors.

Reviewer #4:

Manuscript Summary:

In the manuscript titled with "FLIM-FRET measurements of protein-protein interactions in live bacteria", the authors described a protocol for FLIM-FRET measurements to monitor Protein-Protein Interactions (PPIs) in live Pseudomonas aeruginosa. FRET has been used as a high spatial resolution assay to probe the protein-protein interactions in living cells. The authors demonstrated that FLIM-FRET measurements could be used to characterize the interactions between PvdA and PvdL. Overall, the manuscript is well written, and it fits the scope of the journal. The paper provides detailed protocol for FLIM-FRET measurements. The references also reflect the recent progress in the field.

Major Concerns:

1. Since this choice of FRET pair is critical for FRET measurement, the author should discuss the choice of FRET pair for FLIM measurement.

We do agree that the choice of the FRET pair is a critical point. However, the considerations when using FP pairs is a complex issue that would require a full reviewing - out of the scope of this protocol. To assist the interested reader, we have suggested in the revised version of the manuscript two dedicated references

2. In Fig.2 the authors should provide more details about the biological design of fusion. For example, the linker sequence and length between the fluorescent proteins and PvdA (or PvdL).

Additional information has been added in the plasmid construction section of the protocol

"For PvdA labelled at the C-terminus with eGFP, the 700 bp region upstream relative to the stop codon was amplified by the primers in blue, and the 700 bp downstream region containing the stop codon was amplified with the primers in green. For PvdL labelled at the N-terminus with mCherry, the 700 bp region upstream to the PvdL gene, including the start codon, was amplified by the primers in blue, and the 700 bp downstream region was amplified with the primers in green"

3. Provide brief biological background of PvdA and PvdL to make the report more readable. How stable is the interaction between PvdA and PvdL? What about the binding affinity?

A paragraph has been added in the introduction to provide the biological context of the interaction between PvdA and PvdL.

About the PvdA/PvdL interaction, unfortunately, little is known in term of stability or binding affinity between these two proteins. This is mainly explained by the relative large size of PvdL (480 kDa) - making this protein difficult to express and purify and to be characterized using classical biochemistry experiments.

Minor Concerns:
Give a brief summary about the advantages of FLIM vs other methods for FRET measurement (e.g sensitized emission).

Advantages of FLIM vs other intensity based FRET imaging techniques are discussed in paragraphs 1 and 2 of the discussion

Editorial comments:
You will find Editorial comments and Peer-Review comments listed below. Please read this entire email before making edits to your manuscript.
NOTE: Please include a line-by-line response to each of the editorial and reviewer comments in the form of a letter along with the resubmission.

Editorial Comments:

• Please take this opportunity to thoroughly proofread the manuscript to ensure that there are no spelling or grammatical errors.

*• **Protocol Detail:** Please note that your protocol will be used to generate the script for the video, and must contain everything that you would like shown in the video. **Please add more specific details (e.g. button clicks for software actions, numerical values for settings, etc) to your protocol steps.** There should be enough detail in each step to supplement the actions seen in the video so that viewers can easily replicate the protocol. Some examples:*
1) 2.12: unclear how gentamycin sensitivity is measured.

Done

*• **Protocol Numbering:** Please adjust the numbering of your protocol section to follow JoVE's instructions for authors, 1. should be followed by 1.1. and then 1.1.1. if necessary and all steps should be lined up at the left margin with no indentations. There must also be a one-line space between each protocol step.*

Numbers have been checked

*• **Protocol Highlight:***
1) The highlighting must include all relevant details that are required to perform the step. For example, if step 2.5 is highlighted for filming and the details of how to perform the step are given in steps 2.5.1 and 2.5.2, then the sub-steps where the details are provided must be included in the highlighting.
2) Some of your shorter protocol steps can be combined so that individual steps contain 2-3 actions and maximum of 4 sentences per step.
3) The highlighted steps should form a cohesive narrative, that is, there must be a logical flow from one highlighted step to the next.
4) Please highlight complete sentences (not parts of sentences). Include sub-headings and spaces when calculating the final highlighted length.
5) Notes cannot be filmed and should be excluded from highlighting.

Highlighting was removed for notes - all others points sounds OK

• ***Discussion:*** *JoVE articles are focused on the methods and the protocol, thus the discussion should be similarly focused. Please ensure that the discussion covers the following in detail and in paragraph form (3-6 paragraphs): 1) modifications and troubleshooting, 2) limitations of the technique, 3) significance with respect to existing methods, 4) future applications and 5) critical steps within the protocol.*

• ***References:*** *Please spell out journal names.*

Done

• ***Commercial Language:****JoVE is unable to publish manuscripts containing commercial sounding language, including trademark or registered trademark symbols (TM/R) and the mention of company brand names before an instrument or reagent. Examples of commercial sounding language in your manuscript are (Phusion, ThermoFisher Scientific), (DreamTaq, Olympus IX70, (Insight DeepSee, Spectra Physics , F75-680, AHF, SPCM-AQR-14- FC, Perkin Elmer, (SPC830, Becker & Hickl, SPCImage®,*
1) Please use MS Word's find function (Ctrl+F), to locate and replace all commercial sounding language in your manuscript with generic names that are not company-specific. All commercial products should be sufficiently referenced in the table of materials/reagents._You may use the generic term followed by "(see table of materials)" to draw the readers' attention to specific commercial names.
2) Please remove the registered trademark symbols TM/R from the table of reagents/materials.

Done: all the commercial sounding language has been removed.

• *If your figures and tables are original and not published previously or you have already obtained figure permissions, please ignore this comment. If you are re-using figures from a previous publication, you must obtain explicit permission to re-use the figure from the previous publisher (this can be in the form of a letter from an editor or a link to the editorial policies that allows you to re-publish the figure). Please upload the text of the re-print permission (may be copied and pasted from an email/website) as a Word document to the Editorial Manager site in the "Supplemental files (as requested by JoVE)" section. Please also cite the figure appropriately in the figure legend, i.e. "This figure has been modified from [citation]."*

All figures are original and has not been previously published.